

# Hierarchical Transformers Are More Efficient Language Models

Piotr Nawrot<sup>1\*</sup>, Szymon Tworkowski<sup>1\*</sup>, Michał Tyrolski<sup>1</sup>, Łukasz Kaiser<sup>2</sup>,  
Yuhuai Wu<sup>3</sup>, Christian Szegedy<sup>3</sup>, Henryk Michalewski<sup>3</sup>

<sup>1</sup>University of Warsaw, <sup>2</sup>OpenAI, <sup>3</sup>Google Research  
{p.nawrot99, szy.tworkowski, michal.tyrolski, lukaszkaizer}@gmail.com,  
{yuhuai, szegedy, henrykm}@google.com

## Abstract

Transformer models yield impressive results on many NLP and sequence modeling tasks. Remarkably, Transformers can handle long sequences which allows them to produce long coherent outputs: full paragraphs produced by GPT-3 or well-structured images produced by DALL-E. These large language models are impressive but also very inefficient and costly, which limits their applications and accessibility. We postulate that having an explicit hierarchical architecture is the key to Transformers that efficiently handle long sequences. To verify this claim, we first study different ways to downsample and upsample activations in Transformers so as to make them hierarchical. We use the best performing upsampling and downsampling layers to create Hourglass - a hierarchical Transformer language model. Hourglass improves upon the Transformer baseline given the same amount of computation and can yield the same results as Transformers more efficiently. In particular, Hourglass sets new state-of-the-art for Transformer models on the ImageNet32 generation task and improves language modeling efficiency on the widely studied enwik8 benchmark.

## 1 Introduction

Transformer models (Vaswani et al. 2017) are capable of solving many sequence modeling tasks, including classical NLP tasks (Devlin et al. 2019), summarization (Zhang et al. 2020), language modeling (Radford et al. 2019; Brown et al. 2020), code generation (Chen et al. 2021), or even music generation (Huang et al. 2018; Dhariwal et al. 2020) and image generation (Parmar et al. 2018; Chen et al. 2020; Ramesh et al. 2021). One compelling feature of Transformers is their ability to handle long contexts given as part of the input. This is particularly visible in tasks where the output depends on parts of the context that may not be close-by in the generated sequence, like in summarization, where the summary may need to refer to information scattered across the context, or in large-scale image generation, where pixels belonging to the same object may be far apart in the generation order. Transformers excel at such tasks thanks to self-attention and they are used with longer and longer contexts.

The ability of Transformers to handle long contexts comes at a price: each self-attention layer, at least in its original

\*Equal contribution. Order determined by coin toss.  
Preprint. Under review.

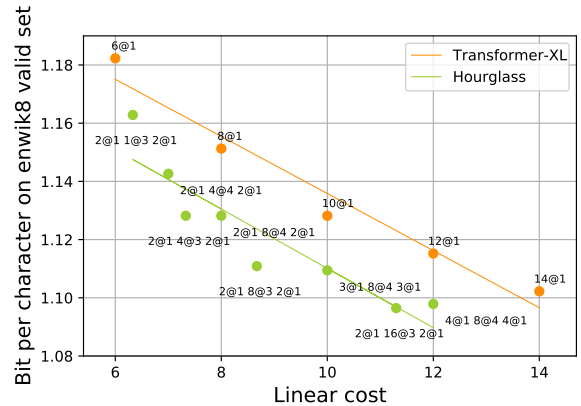


Figure 1: Bits-per-character vs. computation cost for baseline (red) and hierarchical Transformers (green). We observe significant perplexity improvements on enwik8 over the vanilla Transformer-XL baseline, see text for details.

form, has complexity quadratic in the length of the context. When a stack of  $n$  Transformer layers is used, both memory and time complexity is equal to  $O(L^2n)$  where  $L$  is a sequence length and  $n$  number of decoder blocks. Due to this limitation, vanilla transformers are infeasible to train on tasks with very long input sequences, for instance on high-resolution images. This issue has been studied extensively and a number of techniques were introduced that modify attention mechanism without changing overall transformer architecture (Child et al. 2019; Roy et al. 2020; Ren et al. 2021). These sparse attention mechanisms reduce the complexity of self-attention, but still force the model to operate on the sequence of the same length as the input.

For generative Transformer models, operating at the granularity of the input sequence is necessary at least in the early and final layers, as the input must be processed at first and generated at the end (Section 4.2). But forcing the models to operate at this granularity throughout the layer stack has both fundamental and practical shortcomings:

- Fundamentally we aim for the models to create high-level representations of words, entities or even whole events – which occur at a very different granularity than single letters that the model receives on input.

- On the practical side, even layers with linear complexity can be very slow and memory-intensive when processing very long sequences at the wrong granularity.

To alleviate these issues, we propose to change the Transformer architecture to first shorten the internal sequence of activations when going deeper in the layer stack and then expand it back before generation. We merge tokens into groups using a shortening operation (Section 2.1) and so reduce the overall sequence length, and then up-sample them again combining with the sequence from earlier layers (Section 2.3). The first part is analogous to the Funnel-Transformer architecture (Dai et al. 2020) and the whole architecture takes inspiration from U-Nets (Ronneberger, Fischer, and Brox 2015). In contrast to both these architectures, the model we present is autoregressive, which is harder to ensure in hierarchical models than in vanilla Transformers.

The resulting model – which we call *Hourglass* – is an autoregressive Transformer language model that operates on shortened sequences. We show that Hourglass achieves competitive results on benchmarks across various domains. It is the new state-of-the-art among Transformer models for image generation of ImageNet32 (see Tab. 2) and improves perplexity on enwik8 compared to a Transformer-XL baseline (Dai et al. 2019) (see Tab. 1). The comparison to pure Transformer baseline is especially interesting as it shows how the more coarse-grained (higher-level) representations inside the Hourglass layers are not just faster to compute but also superior to the standard fine-grained representations.

## 2 Model

---

Algorithm 1: HourglassLM

---

```

procedure HOURGLASS( $x, [k, \dots, shorten\_factors]$ )
   $x \leftarrow PreVanillaLayers(x)$ 
   $x' \leftarrow Shortening(ShiftRight(x, k - 1), k)$ 
  if EMPTY( $shorten\_factors$ ) then
     $x' \leftarrow ShortenedLayers(x')$ 
  else
     $x' \leftarrow HOURGLASS(x', shorten\_factors)$ 
  end if
   $x \leftarrow x + Upsampling(x, x', k)$ 
   $x \leftarrow PostVanillaLayers(x)$ 

```

---

Figure 3: The architecture starts with *pre vanilla layers* – a stack of Transformer blocks operating on the full token-level sequence. After them we insert *shortening layer* where  $k$  is shorten factor parameter (Fig. 4). The sequence is shifted right before shortening, to prevent information leak (Fig. 5). Then we recursively insert another Hourglass block operating on  $k$  times smaller scale. On the final level of shortening, we apply *shortened layers* – Transformer blocks operating on the smallest scale. *Upsampling layer* brings the resulting activations  $x'$  back to the original resolution. After upsampling and residual, the activations are processed by token-level *post vanilla layers*.

Standard self-attention mechanism uses full token-level sequence representations. In the Hourglass, we bring efficiency to the model by utilizing *shortening*, which allows us to use the Transformer layers on inputs with significantly smaller lengths. A high-level overview of our proposed model architecture is shown in figures 2 and 3.

Attention type in the vanilla layers and shortened layers is a configurable parameter. By default we use relative attention defined in Transformer-XL (Dai et al. 2019). Any attention module can be used - for instance LSH (Kitaev, Kaiser, and Levskaya 2020) which we use for vanilla layers in our experiments on ImageNet64 (see Section 3.3).

### 2.1 Methods of shortening the input sequence

Shortening can be defined as any function  $S$  that accepts a tensor  $x$  of shape  $(l, d)$  and returns a tensor  $x'$  of shape  $(\frac{l}{k}, d)$ , where  $k$  is a hyperparameter called *shorten factor*.

A simple shortening method is 1D average pooling with stride  $k$  and pool size  $k$ , applied along the sequence dimension  $l$ . Another way of shortening is what we will further call *linear pooling* ( $l$  and  $d$  denote sequence length and  $d_{model}$ ):

---

Algorithm 2: LinearPooling

---

```

 $x' \leftarrow Reshape(x, (\frac{l}{k}, k \cdot d))$ 
 $x' \leftarrow LinearProjection(x')$ 

```

---

In this method we first concatenate each  $k$  consecutive token embeddings to get a tensor of shape  $(\frac{l}{k}, k \cdot d)$  and then linearly project its token-dimension back to  $d$  ending up with a tensor of shape  $(\frac{l}{k}, d)$ .

Shortening can be also performed by attention, as was introduced in (Dai et al. 2020):

$$x' = S(x) + Attention(Q = S(x), K = V = x)$$

where  $S$  is shortening function, originally  $S = AvgPool$ . Directly after this attention operation, a positionwise feed-forward with a residual is performed, so that these two layers form a Transformer block (Vaswani et al. 2017). In this work we also try  $S = LinearPool$  and find it more effective on image tasks (see Tab. 6).

### 2.2 Shortening and autoregressive property

**Information leaks** Shortening interferes with the standard causal masking used in Transformer decoders. Namely, in any shortened representation by a factor of  $k$  each shortened token contributes to predicting up to the next  $k$  tokens in the finest scale, that is, if  $e$  is the shortened sequence and  $x$  is the sequence on the finest scale,  $e_0$  is not only used to generate  $x_0$ ; in fact, the same embedding is used to generate tokens  $x_0, \dots, x_{k-1}$ .

Therefore, we need to guarantee that  $e_0$  and any other  $e_i$  cannot access information about tokens they will implicitly predict. To ensure that, we apply another shift right by  $k - 1$  tokens, directly before any shortening by a factor of  $k$  (Fig. 4). The shift is the smallest that does not cause an information leak (see Fig. 5 for an example of a shifting that leads to a leak). We included a more detailed analysis of this fact in the Appendix A.2.

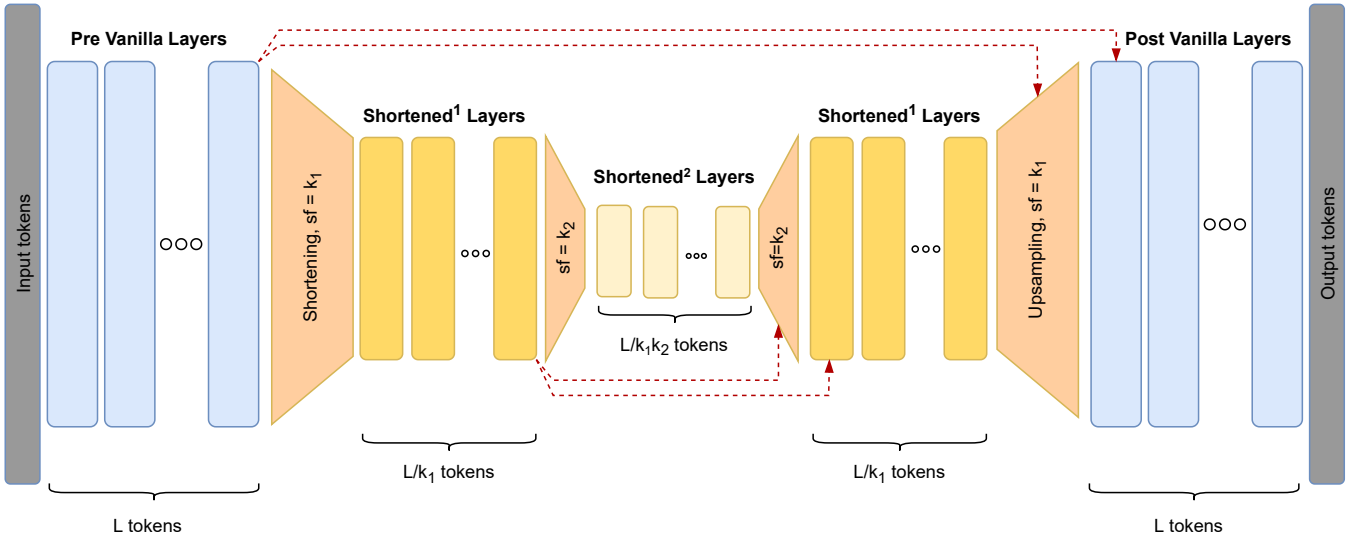


Figure 2: Hourglass - a high-level architecture overview. The arrows denote residual connections.

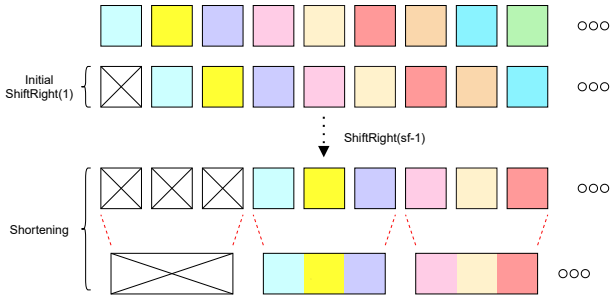


Figure 4: An overview of our shortening approach. Different colors denote token positions. Initially, we shift right by one, which is a standard step in TransformerLM. Then, just before performing shortening, we additionally shift the tokens right by *shorten\_factor* - 1 to preserve the autoregressive property of the model.

**Reduced expressivity** Let consider an Hourglass model with shortening by a factor of  $k$  and no transformer blocks operating on the finest scale (that is a model without vanilla layers).

In this situation  $P(x) = \prod_{i=0}^{n-1} P(x_i | e_0, \dots, e_{\lfloor \frac{i}{k} \rfloor}) = \prod_{i=0}^{n-1} P(x_i | x_0, \dots, x_{\lfloor \frac{i}{k} \rfloor \cdot k - 1})$  because for predicting  $x_i$  we combine the processing done on shortened representations  $e$  with token-independent operations. This means token  $x_i$  is generated independently from the tokens  $x_{\lfloor \frac{i}{k} \rfloor \cdot k}, \dots, x_{i-1}$ . This situation is detrimental to the model's capabilities, though including at least one vanilla layer solves this issue. In the Appendix A.1 we provide a detailed example illustrating this problem.

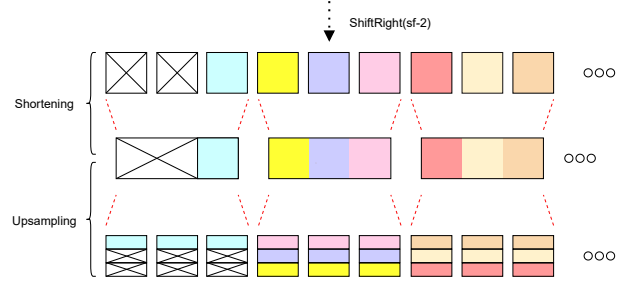


Figure 5: An example of information leak. If the shift right factor is too small then after upsampling the knowledge from the next tokens leaks to previous ones violating autoregressiveness and making decoding impossible. Layers between shortening and upsampling are skipped for clarity and the influence of the attention is omitted for the same reason.

### 2.3 Upsampling methods

Upsampling is a crucial part of the Hourglass architecture since we need to convert shortened representations back to the full token-level sequence in order to perform language modeling. We compare the performance of different upsampling methods in the ablation study in Section 4.

The simplest upsampling method is repeating each shortened vector *shorten\_factor* times as proposed in (Dai et al. 2020). This method is computationally efficient but it does not distinguish with respect to position inside the group. We call it *naive upsampling*.

Another method is *linear upsampling* which works analogously to linear pooling – it projects vectors of shape  $(\frac{l}{k}, d)$  to  $(\frac{l}{k}, k \cdot d)$  and then reshapes to  $l$  vectors, each of dimension  $d$ . This method is fast, memory-efficient and, importantly, it allows to project shortened embeddings differently for each position in the group. This happens because the

$(k \cdot d) \times d$  projection matrix can be thought of as  $k$  separate  $d \times d$  matrices, one per each position.

We also investigated another method which we further call *attention upsampling*. It is similar to attention pooling (Dai et al. 2020) and to the aggregation layer from (Subramanian et al. 2020). It works as follows:

$$x = U(x, x') + \text{Attention}(Q = U(x, x'), K = V = x')$$

where  $x$  are embeddings from just before the shortening,  $x'$  are final shortened embeddings and  $U$  is an arbitrary up-sampling function which accepts  $x$  - embeddings from before the shortening as well as  $x'$  - the shortened embeddings themselves. After the attention operation there is also a residual with a feedforward layer.

Linear upsampling learns a fixed pattern that is the same for each shortened token. Attention upsampling has the advantage of being content-based – each token can extract relevant information from the shortened embeddings. We set:

$$U(x, x') = x + \text{LinearUpsampling}(x')$$

which allows to explicitly inject group-level information into the attention queries. We experimentally show that variants of attention upsampling lead to the best results for our model across different datasets (see Tab. 5).

### 3 Experiments

In this section we compare Hourglass to other models in terms of required running memory, computational cost, and perplexity. We show that by incorporating a single shortening of input we can train larger models in the same budget and achieve better perplexity than the Transformer-XL (Dai et al. 2019) architecture that we will further refer to as our baseline. We use the same relative attention parametrization as Transformer-XL but thanks to shortening we manage to outperform it with the same amount of running memory (Fig. 6).

We applied Hourglass to three language modeling tasks. To show cross-domain generalization of our method we train our model on one dataset related to Natural Language Processing and two from Computer Vision field.

To ensure consistency in presenting configurations of our model, we introduce a notation describing hyperparameters of our architecture:  $(N_1 @ f_1, \dots, N_k @ f_k)$  where each entry  $(N_j @ f_j)$  means  $N_j$  layers shortened by factor  $f_j$ .

Our model implementation and experiment configurations are made publicly available.<sup>1</sup>

#### 3.1 Computational cost analysis

In vanilla Transformers, the number of parameters can be an indicator of the computation required to train the model. This is not true for Hourglass – for instance, it can have 128 layers operating on sequence shortened by 32 and still fit into memory of a single GPU. These layers have the same number of parameters as their vanilla counterparts but are much faster and use less memory.

Hourglass achieves the biggest speedup with the standard  $\mathcal{O}(n^2)$  attention. In that case, a single shortening by

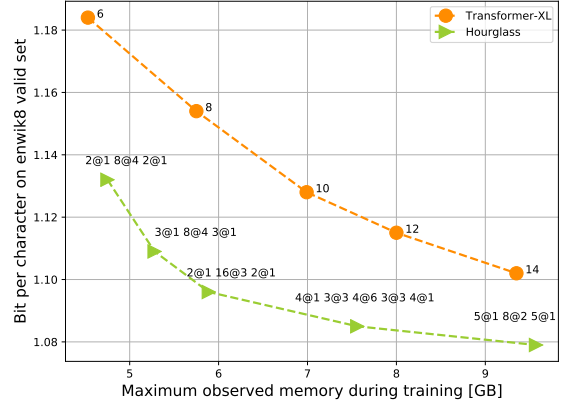


Figure 6: Comparison between Transformer-XL ( $n\_layers$ ) and Hourglass on Enwik8 valid set w.r.t. maximum used memory during training. The results here are evaluated without context using  $seq\ len = 2048$ . Using evaluation with context the  $(5@1, 8@2, 5@1)$  configuration reaches 1.01 bpc on the test set.

a shorten factor  $k$  reduces the complexity to  $\mathcal{O}(\frac{n^2}{k^2})$  so by a factor of  $k^2$ . For more recent linear-time attention mechanisms (Katharopoulos et al. 2020; Choromanski et al. 2021) the reduction would be smaller – but still by a factor of  $k$ . Feed-forward layers also have linear complexity so shortening reduces it by a factor of  $k$ .

This consideration motivates us to use the *linear cost model* for comparisons between different Hourglass configurations and standard Transformers operating on full token-level granularity. In that model, we assume that both attention and feed-forward layers are linear in time and memory with respect to the sequence length. Specifically, to compute the overall cost of a hierarchy we will sum the cost of each transformer layer where layer on the finest level has cost 1 and shortened layers have cost  $\frac{1}{k}$  if they operate on a sequence shortened by a factor of  $k$ . For attention up-sampling/downsampling from  $k_1$  to  $k_2$  scale block we add  $\max(\frac{1}{k_1}, \frac{1}{k_2})$  to the cost. For example, the linear cost of the architecture  $(2@1, 1@2, 4@4, 1@2, 2@1)$  with attention pooling and attention upsampling is  $2 + 1 + \frac{1}{2} + \frac{1}{2} + 4 \cdot \frac{1}{4} + \frac{1}{2} + \frac{1}{2} + 1 + 2 = 9$ .

#### 3.2 Enwik8

Enwik8 (Mahoney 2011) is a byte-level language modeling benchmark containing the first 100M bytes of unprocessed English Wikipedia text, split into 90M train, 5M valid and 5M test sets.

Similarly to (Dai et al. 2019) and (Beltagy, Peters, and Cohan 2020), we evaluate our model on the test set, splitting it into overlapping sequences of size  $l$  with a step size of 128 and calculate the test loss only over the last 128 tokens. With a  $(5@1, 24@3, 5@1)$  hierarchy we reach **0.997** test bpc, evaluated with  $l = 6912$ .

<sup>1</sup>github.com/google/trax/blob/master/trax/models/research/hourglass.py

Enwik8	Cost	BPC
Transformer-XL 12L (Dai et al. 2019)	12	1.06
Adaptive-Span (Sukhbaatar et al. 2019) 12L	12	1.02
BPT (Ye et al. 2019) , seq len = 8192	12	1.02
<b>Hourglass</b> , seq len = 6912	20	0.997
Expire-Span 12L (Sukhbaatar et al. 2021)	12	0.994
Transformer-LS (Zhu et al. 2021)	30	0.97
Feedback Transformer (Fan et al. 2021)	12	0.96
Expire-Span 24L (Sukhbaatar et al. 2021)	24	<b>0.95</b>

Table 1: **Enwik8 Results.** We report bits-per-character (bpc) on the test set and cost in the linear cost model (Section 3.1).

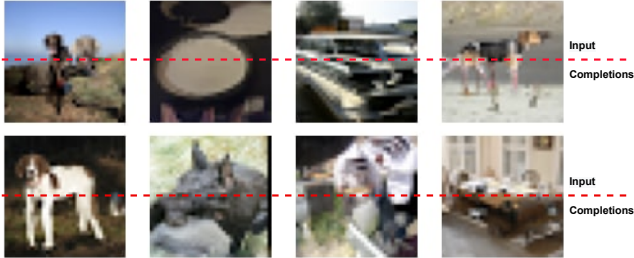


Figure 7: Examples of our model completions, where bottom half of each image was generated by our model, prompted by the upper half.

### 3.3 Image Generation

We use datasets introduced in (van den Oord, Kalchbrenner, and Kavukcuoglu 2016) which are downsampled versions of the popular ImageNet. In the autoregressive image generation setup, they consist of respectively  $32 \times 32 \times 3$  and  $64 \times 64 \times 3$  values per image. As the only preprocessing step, we flatten the images into a 1D sequence.

**ImageNet32** We perform one shortening with factor 3 resulting in 24-shortened-layer model with 3 vanilla layers both at the beginning and the end: (3@1, 24@3, 3@1). We use  $d_{model} = 512$ ,  $d_{ff} = 2048$ , 8 attention heads and 0.01 dropout rate. With this configuration we achieve **3.741** bits/dim, yielding the new state-of-the-art among autoregressive (Transformer-based) models on this dataset, compared to the previous state-of-the-art of 3.758 bpd by (Ho et al. 2019). State-of-the-art for non-autoregressive models is 3.59 bpd achieved by (Kim et al. 2021).

**ImageNet64** Sequence length that our model can handle is limited mostly by the computational complexity of used attention module. To address this problem, in this experiment we verify the compatibility of Hourglass with other attention types. We replace relative attention in vanilla layers by LSH attention (Kitaev, Kaiser, and Levskaya 2020), which allows us to handle **12288**-long sequences. To achieve relative attention parametrization, the LSH attention is combined with rotary positional embeddings (Su et al. 2021). In shortened layers, standard relative attention is used. For LSH attention, we set chunk length to 128 and use 2 hashes, which results in small memory consumption in our full-size

ImageNet32	Cost	BPD
PixelCNN (van den Oord et al. 2016)	-	3.83
Image Transformer (Parmar et al. 2018)	12	3.77
Axial Transformer (Ho et al. 2019)	24	3.76
<b>Hourglass</b>	16	3.74
VDM (Kingma et al. 2021)	-	3.72
UDM (Kim et al. 2021)	-	<b>3.59</b>
ImageNet64	Cost	BPD
Performer (Choromanski et al. 2021)	12	3.64
Combiner-Mixture (Ren et al. 2021)	12	3.50
<b>Hourglass</b>	10	3.44
Sparse Transformer (Child et al. 2019)	48	3.44
Routing Transformer (Roy et al. 2020)	24	3.43
Combiner (Ren et al. 2021)	30	3.42
VDM (Kingma et al. 2021)	-	3.40
UDM (Kim et al. 2021)	-	<b>3.32</b>

Table 2: Bits per Dimension (BPD) on downsampled imagenet. *Cost* denotes linear cost of Transformer model (Section 3.1). Autoregressive models are separated by a horizontal line from non-autoregressive ones. On ImageNet32, our model yields new state-of-the-art for autoregressive models.

layers. In this setup, we reach a score of **3.443** bpd with a (3@1, 12@3, 3@1) architecture which has a total linear cost of 10. All attention layers had  $d_{model} = 768$ ,  $d_{ff} = 3072$  and 8 heads. No dropout was used. Reformer that uses only LSH achieves 3.65 bpd, which shows the contribution of shortened layers.

**CIFAR-10** CIFAR-10 (Krizhevsky 2009) is an image dataset consisting of 60000 images of size 32x32. We use this dataset primarily for our ablations (Section 4). Due to the relatively small number of examples comparing to ImageNet, models reach convergence after 100k steps.

## 4 Ablations

In this section we provide an analysis of Hourglass’ components described above. We start by showing that shortened layers behave similarly to full token-level layers in terms of scalability (Section 4.1). Then we study the effect of different distributions of (*pre*, *post*) vanilla layers on Hourglass’ accuracy (Section 4.2). We further analyze the performance of various upsampling and downsampling methods (Sections 4.4 and 4.3). Finally, we discuss different shorten factors and multi-stage shortening in Section 4.5.

We conduct the ablations on both text and image generation to show applicability across different domains. On enwik8 we train for 200k steps with batch size 8 in each of the ablations. Unless otherwise specified, CIFAR-10 experiments are run for 100k training steps with batch size 8. In both cases we use the Adam optimizer and cosine learning rate schedule with one cycle. Attention and feedforward dropout rate is 0.15 for enwik8, on CIFAR-10 no dropout is used. For the exact hyperparameter setup refer to the Appendix C. In all of the tables, we report bits per character

(BPC) on enwik8 validation (dev) set evaluated without context (sequence length 2048), and bits per dim (BPD) on the CIFAR-10 test set.

#### 4.1 Scaling shortened layers

In this study we want to show that shortened layers - the ones operating on the shortened sequence - contribute significantly to Hourglass accuracy. In Table 3 we evaluate different configurations of Hourglass to measure the impact of scaling the depth of the shortened part of the model. Having fixed the number of vanilla layers we observe perplexity improvements up to 16 layers before saturation or overfitting.

$n$ - number of shortened layers	enwik8	CIFAR-10
Baseline ( $n = 1$ )	1.164	3.28
$n = 4$	1.134	3.16
$n = 8$	1.108	3.07
$n = 16$	<b>1.096</b>	<b>3.03</b>

Table 3: Impact of increasing the number of shortened layers on perplexity. The CIFAR-10 model was trained for 60k steps with total batch size 8, shorten factor = 3 and vanilla layers (1, 1) are fixed for each of the experiments. For enwik8, (2, 2) vanilla layers and shorten factor 3 is used.

#### 4.2 Impact of vanilla layers

We observe a significant contribution to Hourglass’ performance with increasing the number of vanilla layers. One reason is that we perform more computations as in vanilla layers we process the sequence in token-level - no shortening is applied. We also see that the distribution of vanilla layers before shortening and after shortening does impact the training (see Tab. 4) and equal distribution leads to the best perplexity. We show that increasing the number of vanilla layers from (1, 1) to (2, 2) contributes more to the score on enwik8 - it improves from 1.171 to 1.128 bpc, while on CIFAR-10 it is 3.012 comparing to 2.966 bpd (see Tab. 4). We hypothesise that image generation requires less processing of the representations before shortening them, which might be caused by the structure of the input: every 3 consecutive tokens are RGB channels that can be directly grouped into one pixel.

Vanilla layers	enwik8	CIFAR-10
(0, 0)	1.460	3.429
(0, 2)	1.176	3.108
(2, 0)	1.189	3.035
(1, 1)	<b>1.171</b>	<b>3.012</b>
(2, 2)	1.128	2.966

Table 4: Impact of the distribution of vanilla layers on enwik8 (BPC) and CIFAR-10 score (BPD). We see that equal distribution of layers before and after shortening leads to better results on both datasets.

#### 4.3 Upsampling method

In Table 5 we investigate different possibilities of choosing the upsampling method. For attention-free methods, linear upsampling performs better on images, while naive upsampling works well for text. Attention upsampling works well regardless of choice of the function  $U$  and has the lowest perplexity for both images and text.

Upsampling method	enwik8	CIFAR-10
Naive (repeat)	$1.148 \pm 0.001$	3.062
Linear	1.163	3.020
$U(x, x') = x$	1.145	<b>2.967</b>
$U(x, x') = x + \text{Linear}(x')$	<b>1.132</b>	3.012

Table 5: Impact of the chosen upsampling method on valid set BPC on enwik8 with baseline configuration (2@1, 24@4, 2@1). For CIFAR-10 (BPD column) the baseline model hierarchy is (1@1, 8@3, 1@1).

#### 4.4 Pooling method

In this study we investigate the impact of pooling method choice for image and text modalities. Table 6 presents results on both enwik8 (BPC) and CIFAR-10 (BPD). Attention pooling reaches the lowest perplexity for both datasets. Among attention-free methods, average pooling performs well on text, while linear pooling works better for images. Both of these methods perform significantly worse for the other modality. Attention pooling demonstrates small differences with respect to chosen shortening function  $S$  (Section 2.1), still preserving the preference towards linear pooling on images and average pooling on text.

Pooling method	enwik8	CIFAR-10
AvgPool	$1.129 \pm 0.001$	3.116
Attention, $S = \text{AvgPool}$	<b>1.124</b>	3.012
Attention, $S = \text{LinearPool}$	1.142	<b>2.998</b>
LinearPool	1.159	<b>2.998</b>

Table 6: Impact of the chosen pooling method on perplexity. Attention pooling achieves the best score on both datasets.

#### 4.5 Shortening strategies

While the analysis above gives a clear indication of what methods to choose for shortening and upsampling, we are still left with the question of which shorten factors to use and whether to do single-stage or multi-stage shortening.

Unluckily, in contrast to the other ablations, the results on choosing shorten factors are not clear-cut. Consistently, it is beneficial to do at least one shortening and by a factor of at least 3, while keeping 2-3 vanilla layers. Beyond that, a number of different configurations can yield similar results. In Table 7 below we present the different hierarchical configurations that we tested on enwik8 and plotted in Figure 1.

It can be seen that as long as there are not too many vanilla layers (less than 4), the configurations with similar cost perform similarly. The sequence length used in these experiments is 2048 – we hypothesise that more hierarchy may be beneficial with even longer sequences.

Hierarchy	BPC	Linear cost
2@1 4@4 2@1	1.143	7
2@1 8@4 2@1	1.128	8
3@1 8@4 3@1	1.109	10
4@1 8@4 4@1	1.098	12
2@1 1@3 2@1	1.163	6.33
2@1 4@3 2@1	1.128	7.33
2@1 8@3 2@1	1.111	8.66
2@1 16@3 2@1	1.096	11.33
2@1 1@2 4@4 1@2 2@1	1.115	9

Table 7: Different shortening strategies yield similar performance at matching cost with 2-3 vanilla layers.

## 5 Related Work

**Shortening in Transformers** Shortening in our work is inspired by Funnel-Transformer (Dai et al. 2020). The key difference is that they train an encoder model for text classification, where our work is entirely focused on language modeling which provides additional challenges we had to solve regarding shortening in the autoregressive setup (Section 2.2). Another difference is that they use repeat upsampling method while we use attention. There are also a few works related to character-level modeling which use shortening, namely (Xue et al. 2021), (Clark et al. 2021) and (Tay et al. 2021). However, the authors of these works focused mainly on shortening sequence in encoder part of the transformer, whereas we focused on applying shortening in decoder.

The idea of shortening is also discussed in (Subramanian et al. 2020). They propose two architectures: top-down and bottom-up, which also operate on different sequence scales. These architectures however either focus on downsampling or upsampling while Hourglass is a U-Net-like architecture and is symmetric in these terms. In their models, they use transformer layers on the finest scales when postprocessing final representations, we do these also in the beginning to preprocess tokens on the finest scale and we have found it essential to the score (Section 4.2). Our attention upsampling method is similar to their *aggregation layer* in the bottom-up model, however we use one upsampling for each scale change while they combine different scales to create one global upsampling. In contrast to their work, we also use relative attention parametrization.

**Relative positional encoding** Our work is primarily built on the backbone of Transformer-XL (Dai et al. 2019) - we use the same relative attention parametrization. Instead of the segment-level recurrence mechanism proposed in that paper, we use shortening to make our model more efficient

and feasible to train on longer sequences. Another recently proposed relative attention parametrization is RoFormer (Su et al. 2021) where rotary positional embeddings are introduced. We find this work particularly relevant because rotary positional embeddings are compatible with any attention type including efficient attention and can be combined with our model (Section 3.3).

**Sparse Attention** A well-known approach addressing the memory bottleneck is utilizing sparsity patterns in the attention matrix - Routing (Roy et al. 2020) and Sparse Transformer (Child et al. 2019) are examples of such methods. Our solution is different in the sense that it uses full attention - just with shortened sequence length. Combiner (Ren et al. 2021) makes a step further and provides full attention capabilities with similar computational complexity to Routing and Sparse transformers, by leveraging structured factorization. This work, similarly to mentioned above papers on efficient transformers, concentrates on speeding up the attention component, while the most important feature of the Hourglass architecture is that it can use any attention module as a drop-in, including already discussed ones.

**Image generation on downsampled ImageNet** VDM (Kingma et al. 2021) and UDM (Kim et al. 2021) are recently proposed state-of-the-art methods for density estimation on this dataset. The difference between these methods and Transformer-based methods (Parmar et al. 2018; Ho et al. 2019) including this work is that the former are diffusion-based models which unlike Transformers are non-autoregressive.

## 6 Conclusion

In this paper we show how hierarchy can improve efficiency of Transformers in a language modeling setup. Our proposed architecture, Hourglass, significantly outperforms the baseline both in terms of perplexity reached at a given linear computation cost (Figure 1) and empirical metrics like running memory (Figure 6). Hourglass achieves state-of-the-art results among autoregressive models on the ImageNet32 generation task and competitive results on other image generation and language modeling tasks.

Hourglass can be used with any attention type which opens many directions for future research related to Transformers capable of processing longer sequences, improving the tradeoff between efficiency and accuracy. Another line of future work might be related to advances in the shortening mechanism itself, for example involving a dynamic pooling operation that could explicitly handle the problem of fixed-size groups in multi-stage shortening.

We also leave open the problem of choosing the best hierarchy for a task. We conjecture that experiments with much longer contexts will provide better guidance for this choice and will benefit even more from the Hourglass architecture.

## 7 Acknowledgments

Some experiments were performed using the Entropy cluster funded by NVIDIA, Intel, the Polish National Science Center grant UMO-2017/26/E/ST6/00622, and ERC Starting

Grant TOTAL. The work of Henryk Michalewski was supported by the Polish National Science Center grant UMO-2018/29/B/ST6/02959. The authors would like to thank Marek Cygan and Kamil Wilczek for their help with cluster setup, and Grzegorz Grudziński, Dawid Jamka and Sebastian Jaszczur for helpful discussions. This article describes a Team Programming Project completed at the University of Warsaw in the academic year 20/21. We are grateful to Janusz Jabłonowski, the head of Team Programming Projects, for his support and open-mindedness.

## References

- Beltagy, I.; Peters, M. E.; and Cohan, A. 2020. Longformer: The Long-Document Transformer. arXiv:2004.05150.
- Brown, T. B.; Mann, B.; Ryder, N.; Subbiah, M.; Kaplan, J.; Dhariwal, P.; Neelakantan, A.; Shyam, P.; Sastry, G.; Askell, A.; Agarwal, S.; Herbert-Voss, A.; Krueger, G.; Henighan, T.; Child, R.; Ramesh, A.; Ziegler, D. M.; Wu, J.; Winter, C.; Hesse, C.; Chen, M.; Sigler, E.; Litwin, M.; Gray, S.; Chess, B.; Clark, J.; Berner, C.; McCandlish, S.; Radford, A.; Sutskever, I.; and Amodei, D. 2020. Language Models are Few-Shot Learners. arXiv:2005.14165.
- Chen, M.; Radford, A.; Child, R.; Wu, J.; Jun, H.; Luan, D.; and Sutskever, I. 2020. Generative Pretraining From Pixels. In III, H. D.; and Singh, A., eds., *Proceedings of the 37th International Conference on Machine Learning*, volume 119 of *Proceedings of Machine Learning Research*, 1691–1703. PMLR.
- Chen, M.; Tworek, J.; Jun, H.; Yuan, Q.; de Oliveira Pinto, H. P.; Kaplan, J.; Edwards, H.; Burda, Y.; Joseph, N.; Brockman, G.; Ray, A.; Puri, R.; Krueger, G.; Petrov, M.; Khlaaf, H.; Sastry, G.; Mishkin, P.; Chan, B.; Gray, S.; Ryder, N.; Pavlov, M.; Power, A.; Kaiser, L.; Bavarian, M.; Winter, C.; Tillet, P.; Such, F. P.; Cummings, D.; Plappert, M.; Chantzis, F.; Barnes, E.; Herbert-Voss, A.; Guss, W. H.; Nichol, A.; Paino, A.; Tezak, N.; Tang, J.; Babuschkin, I.; Balaji, S.; Jain, S.; Saunders, W.; Hesse, C.; Carr, A. N.; Leike, J.; Achiam, J.; Misra, V.; Morikawa, E.; Radford, A.; Knight, M.; Brundage, M.; Murati, M.; Mayer, K.; Welinder, P.; McGrew, B.; Amodei, D.; McCandlish, S.; Sutskever, I.; and Zaremba, W. 2021. Evaluating Large Language Models Trained on Code. arXiv:2107.03374.
- Child, R.; Gray, S.; Radford, A.; and Sutskever, I. 2019. Generating Long Sequences with Sparse Transformers. arXiv:1904.10509.
- Choromanski, K.; Likhoshesterov, V.; Dohan, D.; Song, X.; Gane, A.; Sarlos, T.; Hawkins, P.; Davis, J.; Mohiuddin, A.; Kaiser, L.; Belanger, D.; Colwell, L.; and Weller, A. 2021. Rethinking Attention with Performers. arXiv:2009.14794.
- Clark, J. H.; Garrette, D.; Turc, I.; and Wieting, J. 2021. CANINE: Pre-training an Efficient Tokenization-Free Encoder for Language Representation. arXiv:2103.06874.
- Dai, Z.; Lai, G.; Yang, Y.; and Le, Q. V. 2020. Funnel-Transformer: Filtering out Sequential Redundancy for Efficient Language Processing. arXiv:2006.03236.
- Dai, Z.; Yang, Z.; Yang, Y.; Carbonell, J.; Le, Q. V.; and Salakhutdinov, R. 2019. Transformer-XL: Attentive Language Models Beyond a Fixed-Length Context. arXiv:1901.02860.
- Devlin, J.; Chang, M.-W.; Lee, K.; and Toutanova, K. 2019. BERT: Pre-training of Deep Bidirectional Transformers for Language Understanding. arXiv:1810.04805.
- Dhariwal, P.; Jun, H.; Payne, C.; Kim, J. W.; Radford, A.; and Sutskever, I. 2020. Jukebox: A Generative Model for Music. arXiv:2005.00341.
- Fan, A.; Lavril, T.; Grave, E.; Joulin, A.; and Sukhbaatar, S. 2021. Addressing Some Limitations of Transformers with Feedback Memory. arXiv:2002.09402.
- Ho, J.; Kalchbrenner, N.; Weissenborn, D.; and Salimans, T. 2019. Axial Attention in Multidimensional Transformers. arXiv:1912.12180.
- Huang, C.-Z. A.; Vaswani, A.; Uszkoreit, J.; Shazeer, N.; Simon, I.; Hawthorne, C.; Dai, A. M.; Hoffman, M. D.; Dinculescu, M.; and Eck, D. 2018. Music Transformer. arXiv:1809.04281.
- Katharopoulos, A.; Vyas, A.; Pappas, N.; and Fleuret, F. 2020. Transformers are RNNs: Fast Autoregressive Transformers with Linear Attention. arXiv:2006.16236.
- Kim, D.; Shin, S.; Song, K.; Kang, W.; and Moon, I.-C. 2021. Score Matching Model for Unbounded Data Score. arXiv:2106.05527.
- Kingma, D. P.; Salimans, T.; Poole, B.; and Ho, J. 2021. Variational Diffusion Models. arXiv:2107.00630.
- Kitaev, N.; Kaiser, Ł.; and Levskaya, A. 2020. Reformer: The Efficient Transformer. arXiv:2001.04451.
- Krizhevsky, A. 2009. Learning multiple layers of features from tiny images.
- Mahoney, M. 2011. Large Text Compression Benchmark.
- Parmar, N.; Vaswani, A.; Uszkoreit, J.; Łukasz Kaiser; Shazeer, N.; Ku, A.; and Tran, D. 2018. Image Transformer. arXiv:1802.05751.
- Radford, A.; Wu, J.; Child, R.; Luan, D.; Amodei, D.; and Sutskever, I. 2019. Language Models are Unsupervised Multitask Learners.
- Ramesh, A.; Pavlov, M.; Goh, G.; Gray, S.; Voss, C.; Radford, A.; Chen, M.; and Sutskever, I. 2021. Zero-Shot Text-to-Image Generation. arXiv:2102.12092.
- Ren, H.; Dai, H.; Dai, Z.; Yang, M.; Leskovec, J.; Schuurmans, D.; and Dai, B. 2021. Combiner: Full Attention Transformer with Sparse Computation Cost. arXiv:2107.05768.
- Ronneberger, O.; Fischer, P.; and Brox, T. 2015. U-Net: Convolutional Networks for Biomedical Image Segmentation. arXiv:1505.04597.
- Roy, A.; Saffar, M.; Vaswani, A.; and Grangier, D. 2020. Efficient Content-Based Sparse Attention with Routing Transformers. arXiv:2003.05997.
- Su, J.; Lu, Y.; Pan, S.; Wen, B.; and Liu, Y. 2021. RoFormer: Enhanced Transformer with Rotary Position Embedding. arXiv:2104.09864.
- Subramanian, S.; Collobert, R.; Ranzato, M.; and Boureau, Y.-L. 2020. Multi-scale Transformer Language Models. arXiv:2005.00581.



Sukhbaatar, S.; Grave, E.; Bojanowski, P.; and Joulin, A. 2019. Adaptive Attention Span in Transformers. arXiv:1905.07799.

Sukhbaatar, S.; Ju, D.; Poff, S.; Roller, S.; Szlam, A.; Weston, J.; and Fan, A. 2021. Not All Memories are Created Equal: Learning to Forget by Expiring. arXiv:2105.06548.

Tay, Y.; Tran, V. Q.; Ruder, S.; Gupta, J.; Chung, H. W.; Bahri, D.; Qin, Z.; Baumgartner, S.; Yu, C.; and Metzler, D. 2021. Charformer: Fast Character Transformers via Gradient-based Subword Tokenization. arXiv:2106.12672.

van den Oord, A.; Kalchbrenner, N.; and Kavukcuoglu, K. 2016. Pixel Recurrent Neural Networks. *CoRR*, abs/1601.06759.

van den Oord, A.; Kalchbrenner, N.; Vinyals, O.; Espeholt, L.; Graves, A.; and Kavukcuoglu, K. 2016. Conditional Image Generation with PixelCNN Decoders. arXiv:1606.05328.

Vaswani, A.; Shazeer, N.; Parmar, N.; Uszkoreit, J.; Jones, L.; Gomez, A. N.; Kaiser, L.; and Polosukhin, I. 2017. Attention Is All You Need. arXiv:1706.03762.

Xue, L.; Barua, A.; Constant, N.; Al-Rfou, R.; Narang, S.; Kale, M.; Roberts, A.; and Raffel, C. 2021. ByT5: Towards a token-free future with pre-trained byte-to-byte models. arXiv:2105.13626.

Ye, Z.; Guo, Q.; Gan, Q.; Qiu, X.; and Zhang, Z. 2019. BP-Transformer: Modelling Long-Range Context via Binary Partitioning. arXiv:1911.04070.

Zhang, J.; Zhao, Y.; Saleh, M.; and Liu, P. J. 2020. PE-GASUS: Pre-training with Extracted Gap-sentences for Abstractive Summarization. arXiv:1912.08777.

Zhu, C.; Ping, W.; Xiao, C.; Shoybi, M.; Goldstein, T.; Anandkumar, A.; and Catanzaro, B. 2021. Long-Short Transformer: Efficient Transformers for Language and Vision. arXiv:2107.02192.

## Appendices

### Appendix A Autoregressive shortening

In Section 2.2 we address two problems of shortening in an autoregressive setup: information leaks and reduced expressivity. Here we study these issues in more detail.

#### A.1 Motivation behind using vanilla layers

At first sight, it may be tempting to create hierarchical models that directly shorten the input to maximize the efficiency gains. In this section, we explain why vanilla layers are crucial for modeling at least some sequences, especially due to autoregressivity.

Consider a sequence modeling task where the input is a random sequence with repeats, such as  $A\#AC\#CD\#DB\#B$ . The sequence consists of chunks  $L\#L$  where  $L$  is a random uniform letter and  $\#$  is a special symbol. A vanilla Transformer language model can achieve 66% sequence accuracy on this task – it cannot predict the token at the beginning

of the chunk, but it can predict the last token of the chunk by simply copying the token at 2 positions earlier, which is possible using a vanilla self-attention layer.

It is however not easy to learn this task in a shortening setup when there are no vanilla layers operating on the finest scale – this is the situation defined in *Reduced expressivity* subsection of Section 2.2. Assume shorten factor is  $k = 3$  and the input is  $A\#AB\#BC\#C$ . To avoid information leak, we shift the input sequence right by 1, and then by  $k - 1 = 2$  directly before shortening. Then the sequence is  $000A\#AB\#B$ . Our shortened embeddings are as follows:  $e_0 = S(emb_0, emb_0, emb_0)$ ,  $e_1 = S(emb_A, emb_\#, emb_A)$  where  $emb$  is input embedding matrix and  $S$  is a shortening function.

Shortened embeddings	[000]	[A#A]	[B#B]
Shifted input embeddings	0A#	AB#	BC#
Target sequence	A#A	B#B	C#C
Positions	123	456	789

Table 8: Example input sequence which is difficult to model without vanilla layers. The model can use only input embeddings shifted by one from the residual and shortened embeddings (shorten factor is 3) to predict the target sequence. Note that it is impossible to predict tokens at positions divisible by 3 using only that information.

Because no vanilla layers are used, for prediction we can use only shortened embeddings and input token embeddings shifted right by 1 from the residual connection. Note that to predict the A token at position 3 we can use only embedding of  $emb_\#$  and  $e_0$  - both of these contain no information so we are unable to predict this token better than randomly (see Table 8). An analogous situation occurs for prediction of any tokens at positions divisible by 3, which makes the model unable to achieve more than 50% accuracy when the task has vocabulary size of at least 2.

This issue can be solved by adding at least one vanilla layer to the model, so that it can attend within the neighborhood of  $k$  previous tokens. For this particular problem, it is sufficient to use local attention with context size  $k$  in vanilla layers which is significantly more efficient than full attention.

#### A.2 Information leaks – analysis

**Definition of an autoregressive model** Formally, given a target sequence,  $x = x_1, \dots, x_n$ , an autoregressive model (e.g. transformer decoder) models the sequence as  $P(x) = \prod_{i=1}^n P(x_i|x_1, \dots, x_{i-1})$  and

$$\forall_i P(x_i|x_1, \dots, x_n) = P(x_i|x_1, \dots, x_{i-1})$$

namely  $x_i$  token depends only on previous tokens, never on itself nor next ones.

**Definition of an information leak** We say that a leak was caused by function  $F_n: A^n \rightarrow A^n$  transforming sequence of input tokens  $(x_1, x_2, \dots, x_n)$

into another sequence  $(u_1, \dots, u_n) = F((x_1, \dots, x_n))$  when  $\exists_{i < j < n} P(x_i | x_1, \dots, x_{i-1}, x_j) \neq P(x_i | x_1, \dots, x_{i-1})$ , namely there exists  $j \geq i$  that token  $x_i$  depends on  $x_j$  which violates the autoregressive property.

**Model representation** Let  $R_k: A^n \rightarrow A^n$  be a shift right function which reindexes tokens by shifting each of them right by  $k$  positions:

$$R_k((x_1, x_2, \dots, x_n)) = (\underbrace{0, \dots, 0}_k, x_1, \dots, x_{n-k})$$

$S_k: A^* \rightarrow A^*$  shortening function with factor  $k$  which takes on input  $x_1, \dots, x_n$  sequence and returns  $s_1, \dots, s_m$  where  $m = \frac{n}{k}$ ,  $U_k$  upsampling function which works in similar way but upsamples  $U_k((u_1, \dots, u_m)) = u_1, \dots, u_n$ .

Between them there is also applied  $D$  decoder function,  $D = D_1 \circ \dots \circ D_l$ , where each  $D_i$  is a function representing decoder block. Due to causal attention masking in the decoder block, there is no risk of information leak caused by function  $D$ .

**Leak description** Because of the mentioned attention mask, we will omit the flow of information between tokens caused by the influence of attention mechanism because this mask keeps the autoregressive property.

Now, let  $(x_1, \dots, x_n)$  be an input sequence and  $(u_1, \dots, u_n) = U(D(S_k(T_s((x_1, \dots, x_n)))))) = F$ . In order to preserve autoregressive property, it is obligatory that no leak occurs.

We will show that shift by any value  $0 < s < k - 1$  where  $k$  is the shorten factor will cause a leak.

To start with, consider input sequence  $(x_1, \dots, x_n)$  and perform operation  $F$ .  $R_s((x_1, \dots, x_n)) = (\underbrace{0, \dots, 0}_s, x_1, \dots, x_{n-s}) = r$ . Assuming that  $n$  is divisi-

ble by  $s$ , we have  $S_k(r) = (v_1, \dots, v_{\frac{n}{k}}) = v$  where each  $v_i$  consists of information obtained in  $(r_{(i-1) \cdot k + 1}, \dots, r_{ik})$ . Now let see that operation  $D$  preserves autoregressive property, let  $d = D(t)$ . Now,  $U(d) = (u_1, \dots, u_n)$  and each  $u_i$  depends on  $d_{\lfloor \frac{i-1}{k} \rfloor + 1}$ .

Now consider  $s \leq k - 2$  and let  $(u_1, \dots, u_n) = F((x_1, \dots, x_n))$  will be a result of our Transformer part. Let take  $u_1$  which depends on  $d_1$  and  $d_1$  depends on  $(r_1, \dots, r_k) = (0, \dots, 0, x_1, \dots, x_{k-s})$ . For that reason  $d_1$  depends on  $x_1, x_2, \dots, x_{k-s}$ , so we have

$$P(x_1 | x_{k-s}) \neq P(x_1)$$

which violates the autoregressive property.

## Appendix B Memory and training time comparison

In Table 9 we show a more detailed comparison between Hourglass and baseline Transformer-XL on enwik8 in terms of running memory (GB) and training steps per second (S) for a given linear cost (C). Running memory and training time for each of the configurations was evaluated on the same Tesla K80 GPU.

Hierarchy	BPC	C	GB	S
6@1 (Baseline)	1.182	6	4.53	0.95
2@1 1@3 2@1	1.163	$6\frac{1}{3}$	4.41	1.11
2@1 4@4 2@1	1.143	7	4.41	1.10
8@1 (Baseline)	1.151	8	5.75	0.73
2@1 4@3 2@1	1.128	$7\frac{1}{3}$	4.88	1.00
2@1 8@4 2@1	1.128	8	4.98	0.99
2@1 8@3 2@1	1.111	$8\frac{2}{3}$	5.50	0.88
2@1 1@2 4@4 1@2 2@1	1.115	9	4.69	0.86
10@1 (Baseline)	1.128	10	6.99	0.56
3@1 8@4 3@1	1.109	10	6.14	0.76
12@1 (Baseline)	1.115	12	8.12	0.47
2@1 16@3 2@1	1.096	$11\frac{1}{3}$	5.89	0.71
4@1 8@4 4@1	1.098	12	7.20	0.62
14@1 (Baseline)	1.102	14	9.35	0.40
5@1 8@2 5@1	1.079	16	9.57	0.45

Table 9: Comparison between Hourglass variants and Transformer-XL baseline on enwik8 – we report validation set perplexity (BPC), linear cost (C), running memory (GB) and training steps per second (S).

## Appendix C Experimental setup

### C.1 Common parameters

Here we list common hyperparameters used for all experiments mentioned in the paper. We use Adam optimizer with  $\beta_1 = 0.9$ ,  $\beta_2 = 0.98$  and  $\epsilon = 1e-9$ . Weight decay and gradient clipping is not used.

In terms of model details, we decided to use a Pre-Norm architecture and FastGelu activation in feed-forward layers.

### C.2 Enwik8

We use  $d_{model} = 512$ ,  $d_{ff} = 2048$  and 8 attention heads. Models in ablation study are trained for 200k steps with cosine learning rate schedule, setting cycle length for 200k steps and linear warmup of 4000 steps. The main result is trained for 260k steps using cosine schedule with cycle length 350k. Dropout rate of 0.2 is used for the main result, while in ablations we use 0.15.

At the beginning of our work on this paper, we have performed grid search over following hyperparameters for enwik8:

- batch size: {8, 16, 32}, finally chosen 8
- dropout: {0.05, 0.1, 0.15, 0.20}, finally chosen 0.15
- learning rate: {1e-4, 2e-4, 3e-4, 4e-4, 5e-4}, finally chosen 4e-4

All next experiments were conducted using these parameters without additional searching, unless otherwise specified.

### C.3 Downsampled ImageNet - common parameters

For ImageNet32 and ImageNet64 experiments we use inverse square root learning rate decay, setting warmup steps to 8000 in both experiments. Total batch size is 64.

## C.4 ImageNet32

In this dataset, we operate on input sequence length of 3072. We use  $d_{\text{model}} = 512$ ,  $d_{\text{ff}} = 2048$ , 8 attention heads and 0.01 dropout rate. We perform 400k training steps with linear warmup and inverse square root decay and then we train for additional 70k steps with cosine learning rate decay, starting from the learning rate from the previous schedule at 400k and decreasing it to 0 at 470k steps.

## C.5 ImageNet64

As an input we receive a sequence of 12288 tokens representing  $64 \times 64 \times 3$  images. We set  $d_{\text{model}} = 768$ ,  $d_{\text{ff}} = 3072$ , 8 attention heads and dropout equal to 0. We perform 300k steps with linear warmup and inverse square root decay.

## C.6 CIFAR-10

All the ablation studies are run for 100k training steps, unless otherwise specified. Input sequence has length 3072 and model parameters are as follows:  $d_{\text{model}} = 512$ ,  $d_{\text{ff}} = 2048$ , 8 attention heads and dropout equal to 0. Total batch size is 8. Cosine learning rate decay with linear warmup of 5000 steps and 100k cycle length is used.

## Appendix D Environment setup

### D.1 Hardware

Experiments are conducted on several setups.

- Ablation Study and short training sessions were computed on nodes consisting of 4x *Titan V* with 12GB memory each, 64GB RAM, *Intel Xeon E5-2660 v4* CPU
- longer trainings were completed on 8x *RTX 2080 Ti* with 11GB memory each, 128GB RAM and *Intel Xeon E5-2660 v4* CPU.
- Few longest trainings were conducted on  $8 \times 8$  TPUv3 units, each with 16GB memory.

### D.2 Software

All experiments were performed on Linux operating system using Trax library version 1.3.9 along with all its dependencies from this particular release date.

## Appendix E Reproducibility

To ensure the reproducibility of this work and to support open science principles, we made our code publicly available at [github.com/google/trax](https://github.com/google/trax). In this repository, we also provide Google Colab notebooks where the evaluation of our main Enwik8 and ImageNet32/64 results can be reproduced.<sup>2,3</sup>

<sup>2</sup>[https://github.com/google/trax/blob/master/trax/models/research/examples/hourglass\\_enwik8.ipynb](https://github.com/google/trax/blob/master/trax/models/research/examples/hourglass_enwik8.ipynb)

<sup>3</sup>[https://github.com/google/trax/blob/master/trax/models/research/examples/hourglass\\_downsampled\\_imagenet.ipynb](https://github.com/google/trax/blob/master/trax/models/research/examples/hourglass_downsampled_imagenet.ipynb)

## E.1 Randomness

Seeds in all experiments were chosen randomly, however each experiment contains history which allows retrieving all randomly set parameters for reproductions.

For each ablation described in the ablation study section, we rerun the baseline 3 times to calculate standard deviation. All other experiments are run only once due to costs and since the variance we noticed was minimal.

## E.2 Experiment representation

Each experiment is represented by a configuration file that unambiguously determines the whole setup – all hyperparameters and training details like specific optimizers, data preprocessing functions, or batch size per device.